Refrigerant selection from an economic and TEWI analysis of cascade refrigeration systems in Europe based on annual weather data

Dario Staubach, Benoît Michel, Rémi Revellin

Refrigerant selection from an economic and TEWI analysis of cascade refrigeration systems in Europe based on annual weather data

Dario Staubach[a], Benoît Michel[a,*], Rémi Revellin[a]

[a] *Univ Lyon, INSA Lyon, CNRS, CETHIL, UMR5008, 69621 Villeurbanne, France*

Abstract

Due to environmental concerns and increasingly stringent regulations, refrigerants with low global warming potential must be used in cascade refrigeration systems. However, identifying the most suitable combination of refrigerants is still a major challenge. Therefore, a methodology for selecting optimal refrigerant combinations for cascade refrigeration systems dedicated to freezing applications is presented. A bilevel optimization procedure approach based on a thermodynamic *0D* steady state model and weather data at different locations in Europe (i.e. France, Germany and Spain) has been developed. The system is optimized in terms of the coefficient of performance on an hourly basis as a lower level task and the total annual cost as an upper level task. The results are analyzed with respect to the annual cost and the corresponding Total Equivalent Warming Impact (TEWI). In total, 36 different low GWP refrigerant pairs were studied for a cascade refrigeration system with an imposed cooling load of 100 kW. The results of the analysis show that dimethyl ether and R161 have the best performance for the high temperature circuit. However, close performances were obtained with R717 and R152a. For the low temperature circuit, similar results were observed for R41, R170 and R744. For the R161/R744 pair, the optimal annual costs and corresponding TEWI are 141 285 €/year and 3001 t, 108 858 €/year and 2459 t, 105 179 €/year and 533 t for Berlin, Madrid

*Corresponding author
Email address: benoit.michel@insa-lyon.fr (Benoît Michel)

and Paris, respectively. Furthermore, the study shows that the optimal refrigerant selection of the investigated refrigerants is robust for the cooled space temperature and the location of the cascade refrigeration system, as no significant change of the TEWI and the total annual cost ranking of the individual refrigerants is observed.

Keywords: cascade refrigeration systems (CRS), refrigerant selection, total equivalent warming impact (TEWI), annual cost, bilevel optimization

---

Nomenclature

Latin Letters

ΔT	Temperature deviation (K)
$\dot{m}$	Mass flow ($\mathrm{kg\,s^{-1}}$)
$\dot{Q}$	Heat rate (W)
$\dot{W}$	Compressor power (W)
A	Area ($\mathrm{m^2}$)
C	Annual costs ($€\,\mathrm{year^{-1}}$)
c	One time costs (USD or €)
COP	Coefficient of performance (-)
CRF	Capital recovery factor (-)
E	Elec. energy consumption (kWh)
GWP	Global warming potential (-)
h	Specific enthalpy ($\mathrm{J\,kg^{-1}}$)
IR	Interest rate (%)
L	Leakage rate ($\mathrm{kg\,year^{-1}}$)
M	Refrigerant charge (kg)
N	Number of years (year)
ODP	Ozone depletion potential (-)
p	Pressure (Pa)
s	Specific entropy ($\mathrm{J\,kg^{-1}}$)
T	Temperature (K or °C)
$TEWI$	Total equivalent warming impact (t)
U	Heat transfer coef. ($\mathrm{W\,m^{-2}\,K^{-1}}$)
x	Vapor quality (-)

Greek Letters

α	Recycling factor (%)
β	Elect. emission factor ($\mathrm{kg\,kWh^{-1}}$)
δ	Pressure ratio (-)
η	Compressor efficiency (%)
γ	Conversion rate ($€\,\mathrm{USD^{-1}}$)
φ	Electricity price ($€\,\mathrm{kWh^{-1}}$)

Indices

c	Circuits; LTC or HTC
$country$	Countries; France, Germany and Spain
hx	Heat exchangers; $evap$, $casc$ and $cond$
p	Points; 1-4

Abbreviations

CRS	Cascade refrigeration system
DME	Dimethyl ether
GWP	Global warming potential
HFC	Hydrofluorocarbons
HFO	Hydrofluoroolefins
HTC	High temperature circuit
LTC	Low temperature circuit
ODP	Ozone depletion potential
TEWI	Total equivalent warming impact

Subscripts

amb	Ambient
$casc$	Cascade
$comp$	Compressor
$cond$	Condenser/Condensation
$cool$	Cool
$crit$	Critical
$direct$	Direct
$elec$	Electrical
$evap$	Evaporator/Evaporation
$heatex$	Heat exchanger
in	Input/Inside
$indirect$	Indirect
inv	Investment
is	Isentropic
LM	Logarithmic
max	Maximum
mix	Electrical and mechanical
obj	Objective variable
out	Output
SC	Subcooling
SH	Superheating

1. Introduction

The refrigeration and air conditioning sector currently consumes about 20 % of the world's electricity production [1]. Due to global warming and the resulting increase in the number of air conditioners and refrigerators in use, the demand for cooling capacities will increase in the coming decades [2]. Moreover, current refrigeration systems still operate with refrigerants that have a high global warming potential (GWP), often around 1000 times that of CO_2, contributing to global greenhouse gas emissions. Limiting the climate impact of a refrigeration system can therefore be achieved both by increasing energy efficiency and by moving to more climate-friendly refrigerants. While the cascade structure of machines is a well-known answer to the first of these problems, especially in food or pharmaceutical freezing applications ($\leq -15\,°C$), the use of CO_2 (R744) as a refrigerant is a very promising answer to the second [3, 4]. However, performance improvements are still desirable and other possible refrigerant candidates are available.

While classical single-stage refrigeration systems are very efficient at moderate evaporator temperatures, two-stage cycles offer a promising alternative at very low evaporator temperatures [3]. In these machines, compression takes place in two successive stages, usually using two different compressors, allowing heat exchange at two different temperature levels. Therefore, this design aims to increase the coefficient of performance (COP) by splitting the compression. There are currently two main families of two-stage machines on the market [5]:

- Flash-Tank refrigeration systems: machines working with only one refrigerant displaced by two compressors, the intermediate pressure being that inside a specific flash tank.

- Cascade refrigeration systems (CRS): machines using two separate refrigerant circuits, which may or may not use the same refrigerant, and which exchange heat through an intermediate cascade heat exchanger.

Although the latter are more complex, sometimes less energy efficient, and more

expensive for high cooling loads than flash tank systems, CRSs have some notable advantages over the latter, in particular:

- The two circuits can be controlled separately and autonomously, giving the whole system flexibility of operation and better adaptability to variations in cooling capacity or ambient temperature. High COP can potentially be achieved over a wider range of cooling capacities.
- The choice of two different refrigerants that can be adapted to the needs of the cooling consumer.

The optimal choice of refrigerant for the low temperature circuit (LTC) and the high temperature circuit (HTC) has been the subject of intensive research in recent years, and various combinations have been studied. For the LTC, R744 is considered a particularly promising candidate because of its good thermodynamic performance and because it is neither toxic nor has a high global warming potential (GWP) [6, 7, 8, 9]. However, its suitability depends on the final application of the CRS and the operating conditions (condensing and evaporating temperatures). Therefore, no general conclusion can be drawn and there are other possible candidates worthy of investigation. Besides R744, R41 and R170 are mainly discussed in other publications as promising candidates for the application in LTC, in some cases surpassing the performance of R744 [3, 10]. Unfortunately, the use of these refrigerants may cause some problems as they are classified in a higher ASHRAE safety class and also have a higher GWP compared to R744.

For HTC, the situation is more complicated because there is an even wider range of possible refrigerants. A comprehensive overview of the refrigerants currently under investigation can be found in Aktemur et al. [11]. Typically, the following refrigerant types are being investigated as potential candidates or are currently in use:

- Hydrofluorocarbons (HFCs) have been used extensively as refrigerants and are still in use because they do not deplete the ozone layer. They were

originally intended to replace chlorofluorocarbons, which deplete the ozone layer. Some have a high GWP and contribute to global warming and must be replaced.

- Hydrofluoroolefins (HFOs) differ from classic HFCs in that they have an unsaturated C-C bond. They have a zero ozone depletion potential (ODP) and a low global warming potential (GWP). R1234yf and R1234zeE are frequently employed, e.g. as a substitution of HFCs [12]. However, it has been reported that they suffer from stability issues [13].

- Ammonia (R717) is one of the oldest refrigerants available and was widely used before the development of chlorofluorocarbons. It is a natural refrigerant with negligible GWP and ODP, the only drawback to its application is its toxicity.

- Hydrocarbons and olefins are non-toxic natural refrigerants with low GWP and negligible ODP. They have interesting thermodynamic properties but are highly flammable. Their application is therefore sometimes problematic and high safety precautions are required.

In consequence, it can be summarized that the discussion about the optimal refrigerant combination has not yet been completely settled.

In the same way as the optimal choice of refrigerants has not yet been conclusively clarified, there are also different criteria according to which the refrigerant selection can be made. Classically, the thermodynamic performance of a CRS can be measured with the COP. Based on the obtained COP, it can be decided whether a refrigerant is suitable for application or not. In addition, other operating parameters of the CRS can be investigated to ensure optimal operation, typically the evaporation or condensation temperature (T_{evap} or T_{cond}) [9, 14]. Experimental results for this approach have been presented, for example, by Sanz-Kock et al. [15] for an R717/R134a CRS. Similarly, Blanco Ojeda et al. [12] experimentally investigated alternative refrigerants (R436A, R1234yf and R513A) to R134a in an R744/R134a CRS. R436A showed an average COP in-

crease of 3.1 %, while R1234yf and R513A showed an average COP decrease of 3.7 % and 4.4 %, respectively.

The analysis of the CRS behavior can be further deepened by an exergy analysis. The goal is to achieve a high COP while providing high exergy output or low exergy destruction [16, 17]. These criteria combined already provide satisfactory refrigerant recommendations. Sun et al. [18] compared combinations of different LTC and HTC refrigerants while varying T_{evap}. They concluded that both R41 and R170 are suitable LTC refrigerants and that R161 is particularly suitable for HTC. Aktemur et al. [11] investigated HTC refrigerants in a R41/HTC CRS at varying T_{evap} and T_{cond} and showed that promising results can also be obtained with DME.

The Total Equivalent Warming Impact (TEWI) is a measure of the global warming contribution of a stationary refrigeration system [19]. Therefore, it is another interesting minimization criterion for the selection of CRS refrigerants. Sánchez et al. [20] calculated and compared the TEWI of a direct expansion R744/R134a CRS and an indirect expansion CRS with different low-GWP refrigerants. They noted that the use of the indirect arrangement significantly reduces the refrigerant mass charge and TEWI. They also stated that R152a would be the most suitable HTC refrigerant for the proposed indirect arrangement. Blanco Ojeda et al. [12] experimentally showed that replacing R134a in an R744/R134a CRS with R436A could significantly reduce the TEWI for Curitiba and Chicago. Adebayo et al. [6] took a different approach and combined TEWI with COP and exergy efficiency to determine the best CRS refrigerant pair. Although they also studied novel fluids such as HFE7000 and HFE7100, they found that the R744/R717 system yielded the highest COP, TEWI, and lowest exergy dissipation of any combination.

However, when selecting a refrigerant based on these criteria, it is important that the underlying models represent the conditions at the intended site well. Realistic results can be obtained if the selected ambient temperature reflects the climatic conditions and is set to the local annual mean temperature [20]. However, even more accurate results can be obtained by considering hourly am-

bient temperature data that reflect daily and annual temperature variations. Bellos and Tzivanidis [13] performed a theoretical analysis of different refrigerants based on hourly weather data of Athens. They concluded that the most efficient refrigerants - from a thermodynamic point of view - are R152a, NH3, R1270, R600, R600a and R290. The authors also suggest verifying these results with additional criteria such as annual costs.

This introduces the last common selection criteria for CRS refrigerant combinations: investment and operating costs can be estimated for a given combination and summarized as annual costs. These annual costs in combination with other selection criteria can be used again to compare different refrigerant combinations or to analyze the CRS performance in detail, e.g. in the form of a combined exergy, environmental and exergo-economic analysis [21, 22, 23, 24]. Another possible application of annual costs is as an objective in a multi-objective optimization, where the goal is to find optimal refrigerants that satisfy several criteria at once [7, 10, 25, 26, 27, 28].

The aim of this work is to present a methodology that allows the selection of refrigerants of CRS dedicated to freezing application (-15 to $-45\,^{\circ}\mathrm{C}$) for different locations in Europe. The proposed refrigerant selection is based on minimized annual cost and corresponding TEWI and reflects local parameters such as country specific electricity price and emission factor. Costs are minimized by varying heat exchanger surface areas on an annual basis and assuming optimal operation of the CRS throughout the year. The thermodynamic properties are calculated with a 0D steady state model on an hourly basis while maximizing the COP to ensure that the assumption of optimal operation is valid. This leads to a bilevel optimization problem for each refrigerant combination using local weather data and other country specific parameters. The proposed methodology is then demonstrated for currently discussed LTC and HTC refrigerants for application in CRSs at different locations in Europe. Our approach is a complementary contribution to the refrigerant selection discussion, as few authors consider local weather data for their analysis. Also, to our knowledge, there is no work that optimizes annual costs by varying heat exchanger areas based on

this weather data. The novelty can therefore be summarized as follows:

- Bilevel optimization approach for optimal COP and annual cost
- Consideration of local parameters like weather data
- Comparison of refrigerant pair performance for different locations in Europe

2. Thermodynamic and mathematical modelling

2.1. System description

The general design of the simulated CRS is depicted in Figure 1. It consists of two separated circuits: one LTC and one HTC. Both circuits incorporate an evaporator, a condenser, an expansion valve and a compressor. They are thermally connected to each other via a heat exchanger in between them, which serves as the condenser for the LTC and as evaporator for the HTC [3]. The

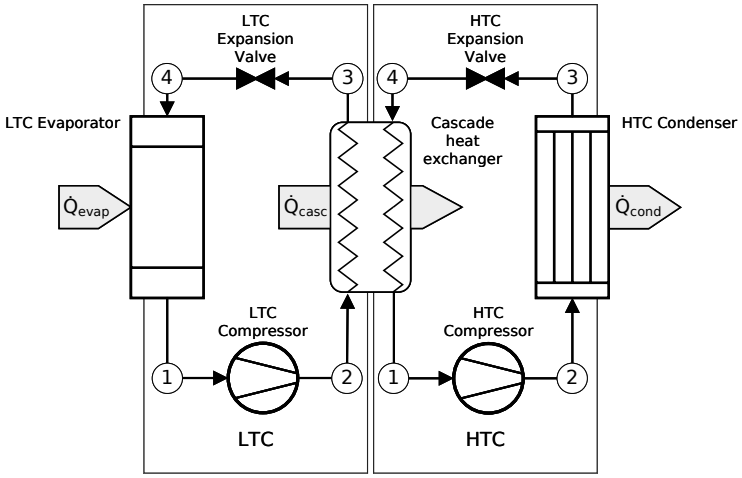

Figure 1: Schematic illustration of the general CRS design.

LTC absorbs the heat $\dot{Q}_{evap}$ and thus is thermally coupled to the cooling space through the evaporator. Starting in the evaporator, the LTC refrigerant evaporates and is already present as superheated vapor at the compressor inlet (Point

1 in Figure 1). Subsequently, the refrigerant is compressed (Point 2) and condenses in the cascade heat exchanger (Point 3). It provides the heat $\dot{Q}_{casc}$ to the HTC during condensation. An adiabatic expansion valve (isenthalpic evolution) closes the cycle and returns the fluid to its initial state (Point 4). The same circulation process takes place in the HTC. The refrigerant of the HTC absorbs the heat $\dot{Q}_{casc}$ in the cascade heat exchanger during evaporation and super heating. The heat $\dot{Q}_{cond}$ is released from the condenser to the ambient air. Therefore, the CRS dissipates heat from the cooled space to the environment at ambient temperature.

An exemplary p-h-diagram of a CRS is shown in Figure 2 to illustrate the overhaul process. Two constant pressure levels within both circuits are clearly identifiable. The remaining indicated points are discussed in Subsection 2.2.

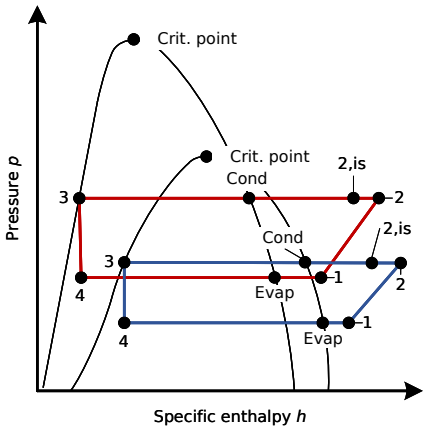

Figure 2: Schematic p-h-diagram of a CRS.

2.2. Thermodynamic model

Based on the system described in subsection 2.1, a *0D*-steady state thermodynamic model of the CRS has been developed and implemented in Python. It utilizes the CoolProp package [29] for the evaluation of the thermodynamic properties and is described below. The main assumptions of the model are as follows:

- All system components are in steady state
- No pressure or heat losses occur through the piping network
- Changes in kinetic and potential energy are negligible
- No subcooling of the liquid in the condensers and only imposed superheating after evaporation in the evaporators ($\Delta T_{SC} = 0\,\mathrm{K}$, $\Delta T_{SH} = 5\,\mathrm{K}$)
- LTC and HTC operate under subcritical conditions
- Only pure or pseudo-pure fluids as refrigerants are employed in both LTC and HTC

Apart from the necessary modeling assumptions, it is important to highlight that the cooling load is fixed at $\dot{Q}_{evap} = 100\,\mathrm{kW}$.

With the assumptions mentioned above, the thermodynamic properties of the refrigerants in LTC and HTC can be determined. The two operating pressures p_1 and p_2 of each circuit can be computed for pure or pseudo-pure fluids as a function of the temperatures T_{evap} and T_{cond}, respectively. The temperatures T_1 and T_3 can be determined taking into account the specified degree of subcooling or superheating, respectively:

$$T_1 = T_{evap} + \Delta T_{SH} \tag{1}$$

$$T_3 = T_{cond} + \Delta T_{SC} \tag{2}$$

With the combinations of temperature and pressure, it is possible to calculate the enthalpy and entropy at any point outside the two-phase region using CoolProp:

$$h_p, s_p = f(T_p, p_1 \text{ or } p_2) \tag{3}$$

According to Figure 2, the pressure p_1 is used for the calculation of point 1 and 4 and the pressure p_2 of point 2 and 3. Within the two-phase region, enthalpy and entropy can be determined by specifying temperature and vapor quality:

$$h_p, s_p = f(T_{evap} \text{ or } T_{cond}, x) \tag{4}$$

The only exception to this scheme is point 2, since temperature, entropy and enthalpy depend on the compressor efficiency. First, the isentropic enthalpy $h_{2,is}$ is determined as $h_{2,is} = f(s_1, p_2)$. Subsequently, the enthalpy h_2 can be calculated as

$$h_2 = \frac{h_{2,is} - (1 - \eta_{is})h_1}{\eta_{is}}, \tag{5}$$

where η_{is} denotes the compressor specific isentropic efficiency.
Based on enthalpies and cooling load, the required mass flow in the LTC can be obtained using

$$\dot{Q}_{evap} = \dot{m}_{LTC} \left(h_{LTC,1} - h_{LTC,4} \right), \tag{6}$$

while the required mass flow in the HTC can be calculated using the transferred heat flow from the LTC to the HTC:

$$\dot{Q}_{casc} = \dot{m}_{LTC} \left(h_{LTC,2} - h_{LTC,3} \right) = \dot{m}_{HTC} \left(h_{HTC,1} - h_{HTC,4} \right) \tag{7}$$

The heat dissipated from the system to the environment can be stated with the following relation:

$$\dot{Q}_{cond} = \dot{m}_{HTC} \left(h_{HTC,2} - h_{HTC,3} \right) \tag{8}$$

2.2.1. Compressor

The electrical power consumption of a compressor can be described as

$$\dot{W}_c = \dot{m}_c \cdot \frac{h_{2,is} - h_1}{\eta_{c,is} \cdot \eta_{c,mix}}, \tag{9}$$

where the parameter $\eta_{c,mix}$ is the combined mechanical and electrical efficiency of the corresponding compressor, which is estimated to be 93 % and does not change throughout the study [7]. Different compressors are used in the LTC and HTC as described in Rezayan and Behbahaninia [8]. According to Petter et al. [30] and Stoecker [31], the isentropic efficiency $\eta_{c,is}$ occurring in Equation 5 and 9 is given for the LTC by

$$\eta_{LTC,is} = 0.00476 \cdot \delta_{LTC}^2 - 0.09238 \cdot \delta_{LTC} + 0.89810, \tag{10}$$

and for the HTC by

$$\eta_{HTC,is} = -0.00097 \cdot \delta_{HTC}^2 - 0.01026 \cdot \delta_{HTC} + 0.83955, \tag{11}$$

with the pressure ratio δ_c defined as:

$$\delta_c = \frac{p_{c,2}}{p_{c,1}} \tag{12}$$

The COP of the CRS is calculated from the LTC and HTC compressor power only, neglecting the electrical consumption of the auxiliaries (e.g. fans). Therefore, the COP is computed as follows:

$$COP = \frac{\dot{Q}_{evap}}{\dot{W}_{LTC} + \dot{W}_{HTC}}. \tag{13}$$

2.2.2. Heat exchangers

In this study, thermal resistance due to heat exchangers is considered. The LTC evaporator and the HTC condenser are assumed to be tube and fine heat exchangers, exchanging heat with the air of the cold space (at T_{cool}) and the ambient air (at T_{amb}), respectively. The cascade heat exchanger is assumed to be a shell and tube heat exchanger. All heat exchangers of the CRS have been separated into different parts in order to take into account significant differences between heat transfer inside the heat exchanger in presence of phase change or not. Thus, they are separated as a function of phenomena: two-phase/two-phase, two-phase/single-phase and single-phase/single-phase. In the case of heat transfer without phase change, a logarithmic temperature difference ΔT_{LM} is applied, while in the case of phase change (i.e. at constant temperature) the difference between the saturation temperatures ΔT is formed. All exchangers are assumed to be adibatic and to operate in counter-flow. Furthermore, both desublimation and dehumidification are neglected. In the following, the process is exemplified on the evaporator:

The total surface area of the evaporator A_{evap} is divided into two parts as presented in Equation 14: the first area $A_{evap,1}$ is needed to evaporate the refrigerant and a second area $A_{evap,2}$ is needed to superheat the fluid.

$$A_{evap} = A_{evap,1} + A_{evap,2} \tag{14}$$

Therefore, the required area for evaporation and for superheating of the fluid must be determined first to calculate the overall surface area of the evaporator:

$$A_{evap,1} = \frac{\dot{Q}_{evap,1}}{U_{evap} \cdot \Delta T} \tag{15}$$

$$A_{evap,2} = \frac{\dot{Q}_{evap,2}}{U_{evap} \cdot \Delta T_{LM}} \tag{16}$$

The heat rates $\dot{Q}_{evap,1}$ and $\dot{Q}_{evap,2}$ can be computed using the already obtained mass flow and corresponding enthalpies for the LTC. In this two parts, the same overall heat transfer coefficient U_{evap} (see Table 1) is used for Equation 15 and 16. Both must sum up to $\dot{Q}_{evap}$:

$$\dot{Q}_{evap} = \dot{Q}_{evap,1} + \dot{Q}_{evap,2} \tag{17}$$

The same procedure can be applied for the cascade heat exchanger and the condenser. For the latter, the cooling and the condensation of the HTC refrigerant has to be considered. Similar to the evaporator, the same overall heat transfer coefficient U_{cond} is used.

Under the assumption that the released heat to cool the LTC refrigerant is always larger than the needed heat to superheat the HTC refrigerant, three different parts can be identified in the cascade heat exchanger:

1. one two-phase/two-phase part corresponding to the HTC fluid evaporation and the LTC fluid condensation
2. one two-phase/single-phase part corresponding to the evaporation of the HTC fluid and the subcooling of the LTC gas
3. one single-phase/single-phase part corresponding to the cooling of the LTC gas and the superheating of the HTC gas

Due to the presence of a gas on at least one side, the heat transfer of the last two parts is limited and the same heat transfer coefficient can be assumed. For simplification, they are combined and considered with a logarithmic temperature difference calculated with the saturation temperatures of both fluids, the LTC input temperature $T_{LTC,2}$ and the HTC output temperature $T_{HTC,1}$. The heat

transfer coefficient U_{casc} is used for the two-phase/two-phase heat transfer while U_{cond} is considered for the combined part.

Note that the U_{hx} of each component depends on the specific heat exchanger design and the observed phase regime of both fluids. To simplify the problem and make it more general, an overall heat transfer coefficient for the entire heat exchanger is used. Typical values are taken from literature for the heat transfer coefficients U_{hx} [10, 21, 28]. However, it is important to emphasize that they are only estimates and are assumed to be the same for all fluids studied for the sake of simplification. The values for the heat transfer coefficients are given by Table 1, whereby the heat transfer coefficients of the condenser and evaporator are related to the external surface area.

Table 1: Heat transfer coefficients taken from literature [10, 21, 28].

Heat exchanger	U_{hx} in $\mathrm{W\,m^{-2}\,K^{-1}}$
Evaporator	30
Cascade heat exchanger	1000
Condenser	40

2.2.3. Validation of the thermodynamic model

The thermodynamic model has been compared with experimental data for a CO_2/R134a CRS from Sanz-Kock et al. [15]. This experimental set up is beyond the scope of this paper, and only its extent of measurements is briefly described here. The authors measured 45 steady-state operating points in total, covering an evaporation temperature range of −40 to −30 °C and a condensing temperature range of 30 to 50 °C. The speed of the compressor was also investigated in detail.

For the purpose of validation, the model has been slightly modified and adjusted to the described experimental setup. The various compressors have been taken into account. Furthermore, the evaporator and the condenser have not been simulated in this comparison. The cascade heat exchanger has been simulated

using an experimental correlation of the HTC and LTC temperature difference as stated in Sanz-Kock et al. [15]. Figure 3 shows the experimentally

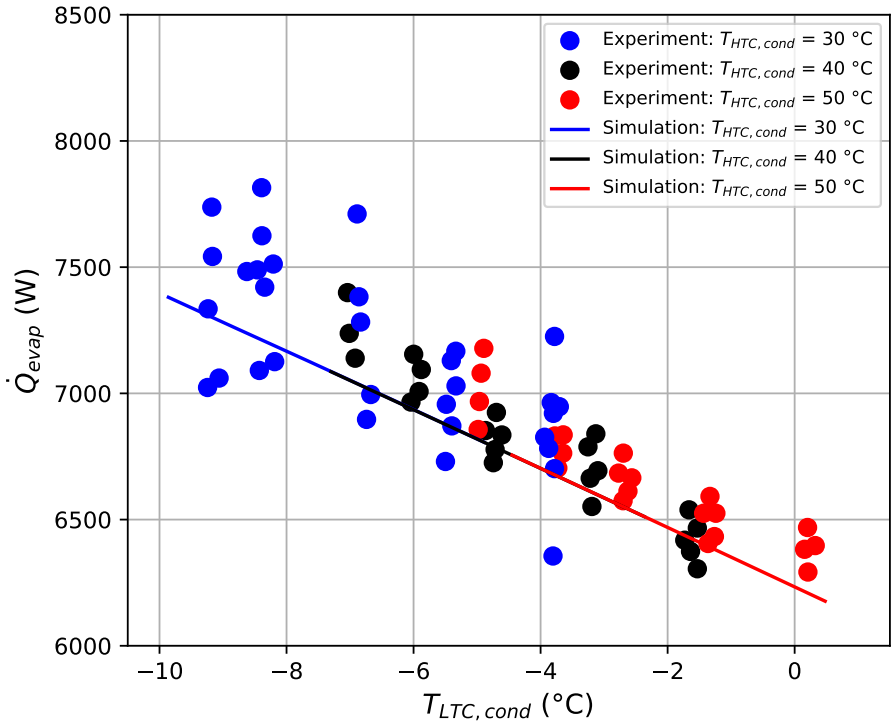

Figure 3: Comparison of simulated and experimentally measured $\dot{Q}_{evap}$ from Sanz-Kock et al. [15].

measured values of the cooling capacity $\dot{Q}_{evap}$ plotted against the condensing temperature $T_{LTC,cond}$. Additionally, the simulated values are in Figure 3 depicted as three straight lines. It can be seen that the experimentally measured cooling capacity $\dot{Q}_{evap}$ of the system decreases as the condensing temperature $T_{LTC,cond}$ increases. Also, the same pattern applies to the condensing temperature $T_{HTC,cond}$. The simulation reflects this behavior. Figure 3 shows that the simulation fits adequately to experimental results, which demonstrated that the thermodynamic model predicts the cascade performances in a satisfactory way. The thermodynamic model is also validated using the COP. In Figure

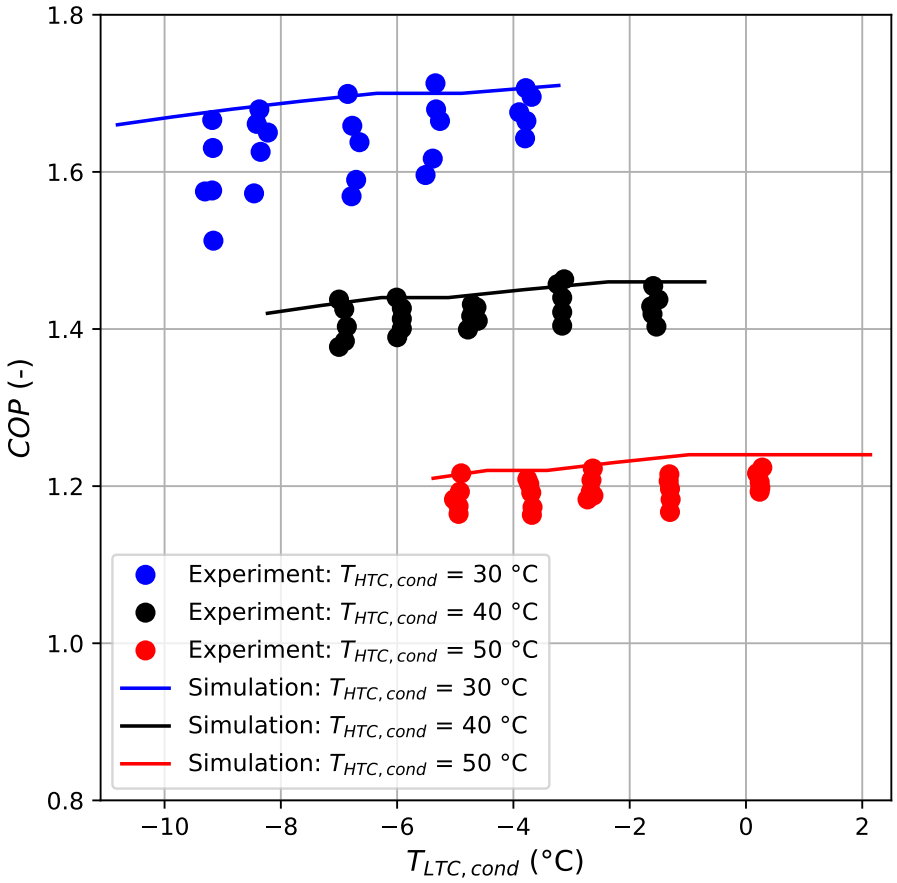

Figure 4: Comparison of simulated and reported COP from Sanz-Kock et al. [15].

4 the reported COP is plotted against $T_{LTC,cond}$ for different $T_{HTC,cond}$. The corresponding simulation results are also shown in Figure 4. As can be seen, the simulation predicts the reported results well.

2.3. Economic analysis

Both investment costs C_{inv} and operating costs C_{elec} are considered for the economic analysis, following the methodology of Rezayan and Behbahaninia [8]. The investment costs involve the purchase of evaporator, condenser, cascade heat exchanger and both the LTC and the HTC compressor. Costs of CRS

auxiliaries and of the refrigerants have not been taking into account. The operating costs include only the electric consumption of the two compressors. The equipment costs for heat exchangers and compressors are given in USD by [32]:

$$c_{heatex} = 1397 \cdot \left(A_{cond}^{0.89} + \cdot A_{evap}^{0.89}\right) + 2382.9 \cdot A_{casc}^{0.68} \tag{18}$$

$$c_{comp} = 9624.2 \cdot \left(\max(\dot{W}_{HTC})\right)^{0.46} + 10167.5 \cdot \left(\max(\dot{W}_{LTC})\right)^{0.46} \tag{19}$$

The variable A_{hx} denotes hereby the effective surface area of the corresponding heat exchanger and $\max(\dot{W}_c)$ the largest encountered compressor capacity within the year. Note that the effective area of the evaporator and condenser is the internal heat exchanger surface area, which must be estimated from the calculated external surface areas. For this reason, an external/internal surface area ratio of 6 is assumed for both [33]. In addition, the prices of the individual components are from the year 2000 and are updated with the CEPCI index as described in equation 20 [32]. The indices used are $CEPCI_{2000} = 391.1$ and $CEPCI_{2022} = 807.7$ [34].

$$c_{2022} = c_{2000} \frac{CEPCI_{2022}}{CEPCI_{2000}} \tag{20}$$

The investment costs are one-time costs that can be converted into annualities. For this purpose, the capital recovery factor CRF is used, which depends on the interest rate IR and the operating time horizon N of the CRS [35]:

$$CRF = \frac{IR \cdot (1 + IR)^N}{(1 + IR)^N - 1} \tag{21}$$

For this study, we set an $IR = 5\,\%$ and a time horizon $N = 15\,\text{year}$ for the plant. This yields $CRF = 0.096$, which means that a loan of $1000\,€$ will be paid back with 15 annual payments of $96\,€$. Furthermore, an estimated conversion factor of $\gamma = 0.833\,€\,\text{USD}^{-1}$ has been multiplied to convert the cost from USD to Euro. This gives us the following expression for the investment costs as anuallities:

$$C_{inv} = \gamma \cdot CRF \cdot (c_{heatex} + c_{comp}) \tag{22}$$

The operating costs solely depend on the electricity consumption of the compressors and the electricity price $\varphi_{country}$:

$$C_{elec} = \varphi_{country} \cdot E \tag{23}$$

The values used for electricity prices $\varphi_{country}$ are presented in Table 2, excluding VAT and other recoverable taxes and levies [36]. The annual energy consumption of the system can be determined by integrating the hourly compressor capacities throughout the year.

Table 2: Electricity prices and country specific CO_2 emission equivalent per kWh for France, Germany and Spain [36, 37].

Country	φ in €kWh^{-1}	β in kg kWh^{-1}
France	0.1042	0.0672
Germany	0.1813	0.4188
Spain	0.1074	0.3043

$$E = \int_{t=0\,\mathrm{h}}^{t=8760\,\mathrm{h}} \left(\dot{W}_{LTC} + \dot{W}_{HTC}\right) \mathrm{d}t \tag{24}$$

With all the above costs, total annual costs for the system can be estimated using the following expression:

$$C_{total} = C_{inv} + C_{elec} \tag{25}$$

2.4. TEWI analysis

In addition to the costs, the impact of the various fluid combinations in the CRS on the environment must also be included in the analysis. A well established and widely used parameter for this purpose is the TEWI. Meaning and calculation method of the TEWI for CRS have already been described in detail in the literature [6, 13, 19, 38, 39]. It indicates the sum of equivalent carbon dioxide emissions for the entire operating time of a system under consideration, but excludes production and recycling. The aim is therefore to obtain a TEWI

that is as low as possible. The TEWI consists of two parts: a direct part and an indirect part of equivalent carbon dioxide emissions.

$$TEWI = TEWI_{direct} + TEWI_{indirect} \tag{26}$$

The direct part of the TEWI is only related to the working refrigerants in CRS. It reflects equivalent carbon dioxide emissions due to leakage and losses during recycling, which are emitted into the atmosphere [19]:

$$\begin{aligned} TEWI_{direct} = {} & GWP_{LTC} \cdot [L_{LTC} \cdot N + M_{LTC}\,(1-\alpha)] \\ & + GWP_{HTC} \cdot [L_{HTC} \cdot N + M_{HTC}\,(1-\alpha)] \end{aligned} \tag{27}$$

The parameter L in Equation 27 depicts the yearly leakage rate and M the total refrigerant charge, both two circuit specific. Note that a recycling factor of $\alpha = 90\,\%$ is assumed for all employed refrigerants and that both LTC and HTC are operating for a number of $N = 15\,\text{year}$. Both parameters are fixed throughout this study. The yearly leakage rate L is proportional to the mass charge M and can be calculated using the following expression [38]:

$$L_c = 0.15 \cdot M_c \cdot \frac{1}{\text{year}} \tag{28}$$

It is assumed that the required circuit specific refrigerant mass charge M_c is proportional to the imposed cooling load $\dot{Q}_{evap}$. The same estimation is used as in Bellos and Tzivanidis [13]: $1\,\text{kg}\,\text{kW}^{-1}$ for the LTC refrigerants and $2\,\text{kg}\,\text{kW}^{-1}$ for the HTC refrigerants. Thus, the mass charge is 100 kg for the LTC refrigerants and 200 kg for the HTC refrigerants. The indirect part of the TEWI is directly related to the yearly electrical power consumption of the system E (Equation 24) and the country specific emission factor $\beta_{country}$ [6, 37]:

$$TEWI_{indirect} = E \cdot \beta_{country} \cdot N \tag{29}$$

3. Methodology

In this study, different refrigerant combinations are systematically analyzed and compared at different locations in Europe based on annual costs and corresponding TEWI. We briefly present the refrigerants studied and the weather

data used during optimization. Subsequently, the bilevel optimization formulation is introduced.

3.1. Investigated refrigerants

Three different low temperature refrigerants and twelve high temperature refrigerants were selected, making a total of 36 possible combinations. All refrigerants investigated have an ODP of zero and an already comparatively low GWP [40, 41, 42, 43] according to the current European F-gas regulation [44], which prohibits the usage of fluorinated greenhouse gases with a GWP ≥ 2500. The criterion of a GWP ≤ 150 for new systems on the European market is also met, except from R134a, R32 and RE143a. These refrigerants, with their corresponding GWP, refrigerant type, ASHRAE safety group ([45, 46]) and critical temperature, are presented in Table 3 and 4. Please note that we have declared Hydrocarbons and -olefins, R744 (CO_2) and R717 (NH_3) in those tables combined as natural refrigerants.

Table 3: List of low temperature refrigerants. Note that the temperatures are given in °C and the enthalpy of evaporation Δh_{LV} (at $-30\,°C$) in $kJ\,kg^{-1}$

Refrigerant	Type	T_{min}	T_{crit}	Δh_{LV}	Safety group	GWP	Sources
R744	Natural	-56.6	31.0	303.5	A1	1	[40, 45]
R170	Natural	-182.8	32.2	388.8	A3	6	[40, 45]
R41	HFC	-143.3	44.1	406.9	A2	116	[41, 46]

Table 4: List of high temperature refrigerants. Note that the temperatures are given in °C and the enthalpy of evaporation Δh_{LV} (at 0 °C) in kJ kg^{-1}

Refrigerant	Type	T_{min}	T_{crit}	Δh_{LV}	Safety group	GWP	Sources
R717	Natural	-77.7	132.3	1262.2	B2l	0	[42, 45]
R290	Natural	-187.6	96.7	374.9	A3	3	[40, 45]
R600	Natural	-138.3	152.0	385.3	A3	4	[40, 45]
R1270	Natural	-185.2	91.1	377.6	A3	2	[40, 45]
RE170/DME	Natural	-141.5	127.2	435.0	A3	1	[40, 45]
R1234yf	HFO	-53.2	94.7	163.3	A2l	4	[43, 45]
R1234zeE	HFO	-104.5	109.4	184.2	A2l	6	[43, 45]
R161	HFC	-143.2	102.1	379.0	A3	4	[41, 46]
R152a	HFC	-118.6	113.3	307.1	A2	138	[41, 45]
R134a	HFC	-103.3	101.1	198.6	A1	1300	[41, 45]
R32	HFC	-136.8	78.1	315.3	A2l	677	[41, 45]
RE143a	HFC	-33.2	104.8	198.0	-	756	[40]

3.2. Weather data and cities studied

Hourly temperature data for an entire year is utilized to account for the climate conditions at each city studied [47]. The data therefore reflects how many hours an ambient temperature T_{amb} is present per year. This information can be used to simulate the behavior of the CRS for each ambient temperature and to scale it up to the whole year. As a graphical example, the weather data for the city of Lyon is shown in Figure 5. Weather data of a total of four cities in France, Germany and Spain has been utilized in this work, which is given in Table 5. In addition to the minimum and maximum temperature, the average temperature and the temperature ranges, in which the temperature varies over the whole year, are also indicated. These cities were chosen to have a sufficiently warm climate on the one hand and different electricity prices φ and electricity emission factor β on the other (Table 2). Therefore, conclusions about the influence of these parameters can be drawn later by comparing the obtained results for refrigerant combinations.

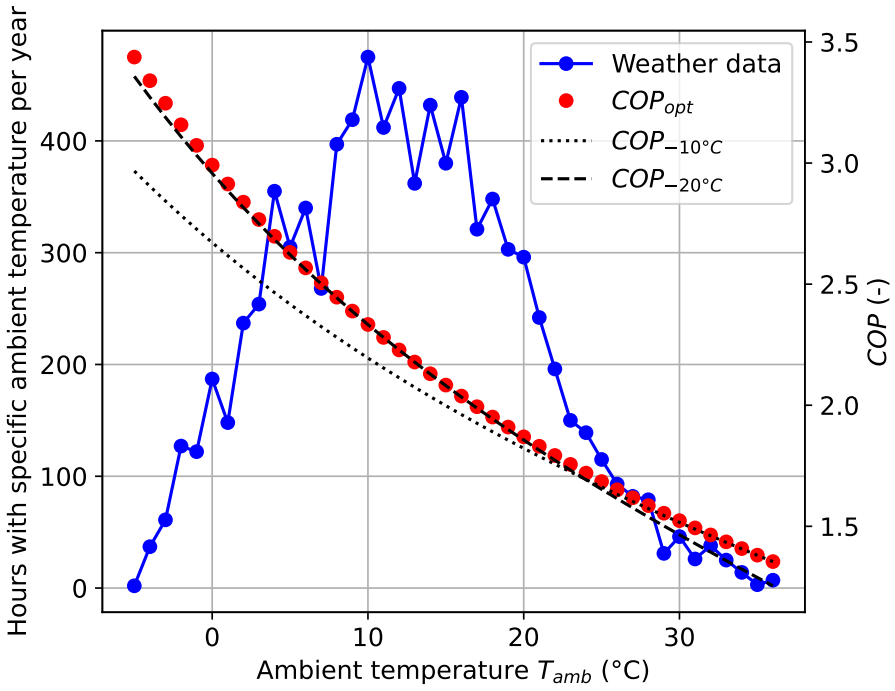

Figure 5: Weather data for Lyon and corresponding hourly COP for different operating conditions.

Table 5: List of investigated cities with corresponding temperature information.

City	Country	T_{min}	T_{mean}	T_{max}	ΔT_{range}
Berlin	Germany	−11 °C	9.2 °C	34 °C	45 K
Paris	France	−7 °C	10.7 °C	35 °C	42 K
Lyon	France	−5 °C	12.3 °C	36 °C	41 K
Madrid	Spain	−6 °C	12.1 °C	36 °C	42 K

3.3. Optimization

In this paper, optimal annual costs and corresponding TEWI of different refrigerant combinations are analyzed and compared. Those quantities are influenced by the heat exchanger surface areas, which are in consequence chosen as objective variables. Annual costs and TEWI should, however, be computed

under the assumption of optimal operation of the CRS and thus optimal annual COP. This implies that the COP has to be maximized for every occurring T_{amb}, varying the condensation temperature $T_{LTC,cond}$. Therefore, a bilevel optimization has to be carried out. Hereby, minimization of annual costs is the upper-level optimization task and the maximization of the hourly COP represents the lower-level optimization task. Both optimization problems are solved with *scipy.minimize* [48], the lower-level task applying the *trust-constr* algorithm [49] and the upper-level task using *Powell's* method [50]. A schematic representation of the optimization procedure is presented with Figure 6.

Upper-level task: annual costs. Annual total costs are minimized for a given set of refrigerant combination by varying heat exchanger surface areas $A_{obj} = [A_{evap}, A_{casc}, A_{cond}]$. Consequently, the optimization problem in terms of costs can be stated as follows:

$$\min_{A_{obj}} \quad C_{total} \tag{30}$$

The optimization variable bounds are given in Table 6. Note that varying the surface areas also influences the COP. So, to ensure optimal operation of the CRS, the annual COP has to be maximized for each iteration in a lower-lever optimization.

Table 6: Upper and lower bounds of the surface areas.

Objective variable	A_{evap}	A_{casc}	A_{cond}
Lower bound	$100\,\mathrm{m}^2$	$35\,\mathrm{m}^2$	$100\,\mathrm{m}^2$
Upper bound	$1000\,\mathrm{m}^2$	$200\,\mathrm{m}^2$	$1000\,\mathrm{m}^2$

Lower-level task: hourly COP. To ensure optimal operation throughout the year, the COP must be maximized for each occurring ambient temperature. The appropriate operating temperatures have to be determined as objective variables given by:

$$T_{obj} = [T_{LTC,evap}, T_{LTC,cond}, T_{HTC,evap}, T_{HTC,cond}]$$

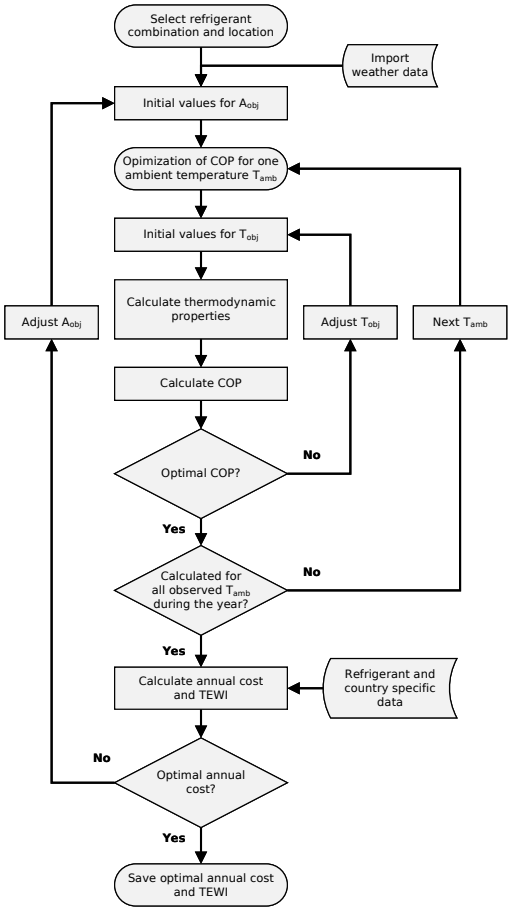

Figure 6: Flow chart of the annual costs optimization algorithm.

At the same time, constraints imposed by given heat exchanger areas must be fulfilled, resulting from the upper-level task. A constraint is introduced for each heat exchanger so that the sum of the two partial areas is equal to the total heat exchanger surface area (constraints 31b-31d). Additional constraints are introduced to ensure that the temperature difference between condensation and evaporation temperature are smaller than 2.5 K (constraints 31e and 31f) and that $T_{LTC,cond}$ is always higher than $T_{HTC,evap}$ (constraint 31g). Upper and lower bounds of the temperatures depend on the utilized refrigerants and their supported temperature in CoolProp [29]. Thus, the associated optimization

problem related to optimal operation can be stated for a given set of heat exchanger areas as follows:

$$\max_{T_{obj}} \quad COP \tag{31a}$$

$$\text{s.t.} \quad A_{evap} - \sum_{i=1}^{2} A_{evap,i}(T_{obj}) = 0, \tag{31b}$$

$$A_{casc} - \sum_{i=1}^{2} A_{casc,i}(T_{obj}) = 0, \tag{31c}$$

$$A_{cond} - \sum_{i=1}^{2} A_{cond,i}(T_{obj}) = 0, \tag{31d}$$

$$T_{LTC,evap} - T_{LTC,cond} + 2.5 < 0, \tag{31e}$$

$$T_{HTC,evap} - T_{HTC,cond} + 2.5 < 0, \tag{31f}$$

$$T_{HTC,evap} - T_{LTC,cond} < 0 \tag{31g}$$

3.4. Limitations of the proposed methodology

In this section, we want to address the limitations of the presented methodology. First, an obvious limitation is the use of a steady-state model to simulate the thermodynamic behavior of the CRS throughout the year. This is particularly the case due to the rapid changes of the weather, which can only be represented by a dynamic model. However, the weather data is provided on an hourly basis and the observed hourly temperature fluctuations are small. Therefore, the steady-state results serve as an approximation for the proposed methodology. Further limitations result from the listed assumptions of the thermodynamic model. In addition, the constant heat transfer coefficients and the same imposed refrigerant mass charge for all operating conditions and different refrigerants are only estimates that allow comparison of a wide range of different refrigerant pairs. Therefore, the results are not generally accurate, but their trends are still valid and meaningful.

4. Sensitivity analysis

A sensitivity analysis of the objective variables on the objective functions of the bilevel optimization was carried out. The aim of the analysis is to describe the influence of condenser temperature $T_{LTC,cond}$ and surface areas on the CRS behavior and their impact on COP and annual costs. During this analysis, the LTC is employed with CO_2 while the HTC is employed with NH_3. The cooled space temperature T_{cool} is set to $-30\,°C$ and the evaporation temperature to $T_{LTC,evap} = -40\,°C$. The city of Lyon is chosen as example for the analysis.

4.1. Sensitivity analysis of the lower-level task

As a first step, the influence of the condenser temperature $T_{LTC,cond}$ on the CRS performance is studied. To do so, two simulations are performed imposing a different but constant $T_{LTC,cond}$ ($-10\,°C$ and $-20\,°C$) throughout the year, and corresponding COP are computed on an hourly basis. These COP values are plotted against the corresponding T_{amb} and compared to the COP obtained using an optimal $T_{LTC,cond}$ in Figure 5. The surface areas are fixed, A_{evap} and A_{cond} both at $400\,m^2$ and A_{casc} at $75\,m^2$. We show in the following paragraph, that those values are typical for the system at hand and not far away from the optimum regarding annual costs.

The COP obtained using the optimal condenser temperature $T_{LTC,cond}$ is, as expected, always larger than the other two COP over the entire temperature range. However, it can also be clearly seen that the optimum condensing temperature changes over the ambient temperature curve. In contrast, the curve of $T_{LTC,cond} = -20\,°C$ approaches the optimal COP for T_{amb} close to $10\,°C$ and then drops off. The curve of $T_{LTC,cond} = -10\,°C$ approaches also an optimum COP for $T_{amb} \geq 30\,°C$. Thus, it can be shown that the selection of a suitable condensing temperature $T_{LTC,cond}$ for each T_{amb} compared to a fixed value for $T_{LTC,cond}$ can ensure better performance of the CRS throughout the year.

4.2. Sensitivity analysis of the upper-level task

The next step is to investigate the influence of heat exchanger surfaces on annual costs and COP. We have chosen to use COP rather than TEWI because they are directly correlated. A corresponding figure would therefore show the same trend for both. For this purpose, both the cascade heat exchanger and the condenser surface areas are varied over a range of 40 to 160 m^2 and 200 to 800 m^2, respectively, while the evaporator surface area is fixed at 400 m^2. The missing temperatures are calculated by solving the lower-level task.

The corresponding heatmap of the COP and annual costs are depicted in Figure 7. Figure 7a shows that the COP is obviously increasing for both increasing A_{casc} and A_{cond}. This observation isn't surprising since larger surface areas allow for smaller driving temperature differences. As a consequence, the COP would reach its maximum value at infinitely small driving temperature differences, respectively at infinitely large heat exchange surfaces. For the TEWI, this means that it reaches its minimum at infinitely large heat exchange surfaces. A completely different behavior can be observed in Figure 7b: annual costs clearly have an optimum. Also, a predominant dependency of the area A_{cond} can not be observed since both areas have a significant influence on annual costs. However, in comparison to Figure 7, it is important to highlight that the optimum of the costs does not correspond to an optimum of COP or TEWI.

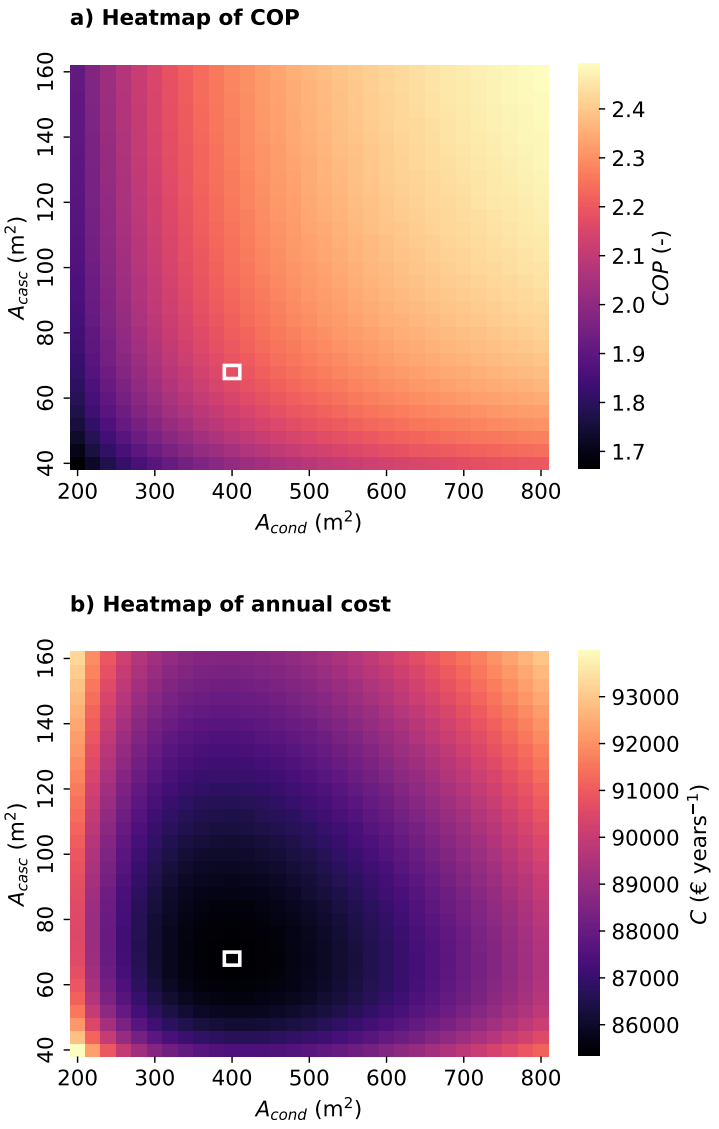

Figure 7: Comparison of the calculated COP and Costs for Lyon. The optimal combination of surface areas regarding annual costs is marked in white in both subfigures.

5. Results and discussion

The results are presented as a comparison of TEWI and optimal annual costs incurred for the operation of a refrigerant combination. We begin by discussing results for HTC refrigerants in three different cities and continue with more specific analysis for the city of Paris. Subsequently, LTC refrigerants candidates are discussed and analyzed.

5.1. Analysis of different HTC refrigerants

A comparison of optimal solutions found regarding annual costs is presented for the capitals Berlin, Paris and Madrid. R744 is employed as LTC refrigerant in the CRS at hand. Figure 8 depicts the obtained results as annual costs versus TEWI at $T_{cool} = -45\,°\mathrm{C}$. The complete dataset is available in the Appendix (Table 8).

First, the different ranges of annual costs and corresponding TEWI are analyzed and compared for all three cities. For a better overview, minimum, maximum and the deviation between maximum and minimum values in percents of the observed variables are given by Table 7. As indicated in Table 7, all refrigerant combinations in Berlin have a considerably higher annual cost rate than all combinations in Paris and Madrid, where they are about the same range. In addition to the annual costs, the TEWI is significantly larger in Berlin compared to Paris, whereas it is a bit smaller in Madrid. Both effects can be explained by the underlying parameters. Since annual costs are optimized, country-specific electricity prices have a particular impact on the results. As indicated in Table 2, electricity prices are about the same in France and Spain. In Germany, the electricity price is substantially more expensive. Therefore, it is not surprising that the annual cost margins differ and the highest annual cost rate is obtained for the city of Berlin. This is in contrast to the annual mean temperatures, as they are in both Paris and Madrid higher than in Berlin, implying an increased electricity demand for cooling. The same is valid for the TEWI. In both Germany and Spain, electricity emission factor β is considerably higher

than in France, as already highlighted in Table 2. This also explains low values for the TEWI in Paris in contrast to high values obtained for Berlin and Madrid. The observed maximal annual costs variation between the best and

Table 7: Annual costs and TEWI range comparison for Berlin, Madrid and Paris.

	Berlin	Madrid	Paris
Max C (€ year^{-1})	146715	113814	109758
Min C (€ year^{-1})	141256	108858	105179
Max Deviation of C (%)	3.9	4.6	4.4
Max $TEWI$ (t)	3666	3115	1151
Min $TEWI$ (t)	2988	2447	529
Max Deviation of $TEWI$ (%)	22.7	27.3	117.6

worst performing HTC refrigerant is for all three cities low and approximately the same. This is not the case for the maximal TEWI deviation: it is high for all three cities, even reaching a value of 117.6 % in Paris. We can therefore conclude that attention should be paid to the TEWI when selecting the refrigerant for a specific location, as a high variation is detected here.

Another interesting observation is the individual HTC refrigerant performance and the way they are distributed in Figure 8. For a better overview, the HTC refrigerants are grouped into three different sets based on their types: natural refrigerants (R717 R290, R600, R1270, DME), HFC (R161, R152a, R32, RE143a, R134a) and HFO (R1234yf, 1234zeE).

We first consider the natural refrigerants. These refrigerants are often not employed because of their safety classification, for example due to high flammability or toxicity. Nonetheless, there is recently a growing interest in them as they show very interesting properties. In all the cities shown in Figure 8, the annual costs ranking is as follows: DME with the lowest cost, closely followed by R1270 and later by R290, R717 and R600. The group internal annual cost deviation is in the same range as for the HFC and all natural refrigerants yield lower annual costs as the HFOs. Regarding TEWI, an almost same refrigerant ranking can

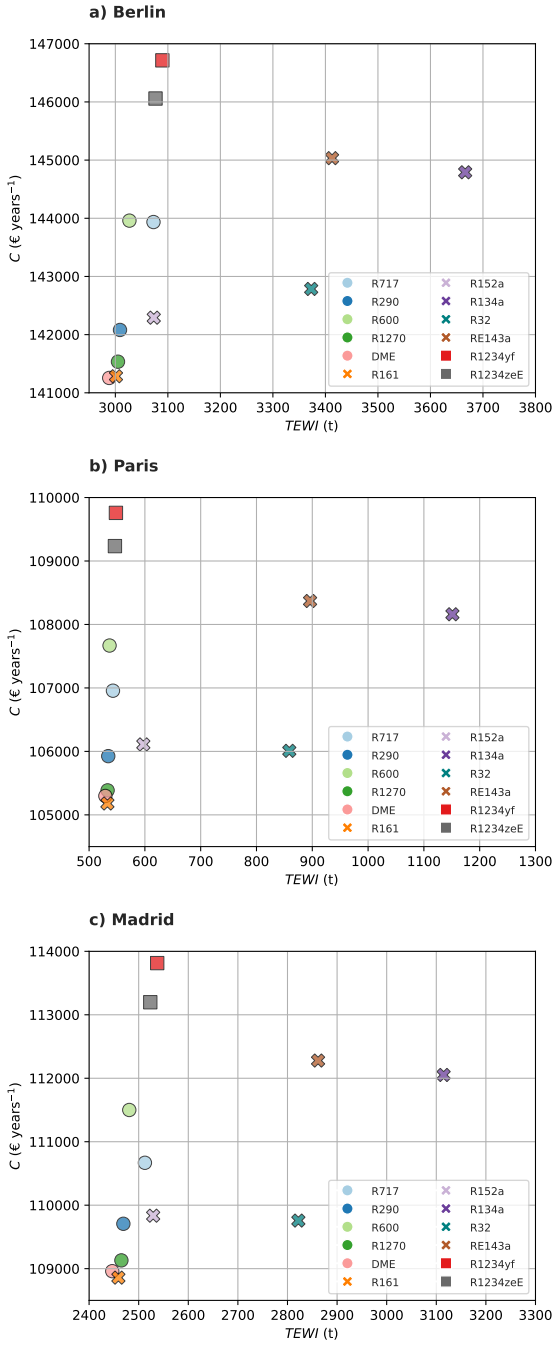

Figure 8: Optimal annual costs of R744/HTC refrigerant combinations for the cities of a) Berlin, b) Paris and c) Madrid for a cooled space temperature $T_{cool} = -45\,°C$. Circles indicate natural refrigerants, crosses HFC and squares HFO.

be seen. Instead of R600, R717 has the highest TEWI of the natural refrigerants while DME provides the lowest TEWI of all refrigerants studied. Nevertheless, TEWI variation is very small, and all natural refrigerants studied are suitable from this point of view. Because of the aforementioned high flammability, their use might be limited due to safety concerns. R717 is the only natural refrigerant considered in this paper that is not in ASHRAE safety group A3. Since it is toxic, all refrigerants of this type can only be used with appropriate safety precautions.

Next, the HFC are considered. A high variation in both annual cost and TEWI is observed for this refrigerant type in all cities. The annual costs ranking is as follows: R161 corresponds to the lowest annual costs of all refrigerants studied, followed by R32, R152a, R134a and RE143a. A similar ranking can be seen for the TEWI: R161 has the lowest TEWI of this type, however, it is followed by R152a, R32, RE143a and R134a being the refrigerant with the highest TEWI of all refrigerant studied. Thus, R161 is a promising refrigerant. It is, however, also in ASHRAE safety group A3 and appropriate safety precautions are necessary. R152a and R32 are also suitable, the first due to its low TEWI and the latter due to being the flammable refrigerant studied with the lowest annual costs. Because of their very high TEWI and high annual costs, both RE143a and R134a cannot be recommended.

Lastly, we consider the HFO R1234zeE and R1234yf. They have both considerably small TEWI, but correspond to the most expensive configuration studied, with R1234yf performing slightly worse in terms of annual costs and TEWI. Even through R1234zeE and R1234yf indicate the highest annual costs, the deviation regarding optimal total annual costs is comparatively low (3.9 to 4.6 %) and both might serve as good HTC candidates. The behavior of HFOs in CRS resembles to the behavior of HFC (e.g. same pressure range) and it is not necessary for CRS manufacturers to change the overall design.

A comparison of the rankings between the individual types and cities also shows almost no difference, only one displacement can be detected. The TEWI performance ranking is the same for Berlin and Madrid. In Paris, however, a

deviation from this ranking can be observed: here, R1234zeE, and R1234yf have both lower TEWI than R152a. This observation can be explained by the fact that R152a has a comparatively high GWP. Since the electricity emission factor β is very low in France, the good performance cannot compensate for the direct contribution to the TEWI due to uncontrolled emission of the refrigerant into the atmosphere. This is not the case for Berlin and Madrid, where the electricity emission is significantly higher than in Paris. As a consequence, the direct part of the TEWI in Berlin and Madrid is comparatively low and is not decisive for the TEWI. In summary, high variation of annual costs and TEWI can be detected for the same refrigerant combinations at different locations. Nevertheless, the performance ranking is only slightly influenced, which implies that the refrigerant recommendations can be made to a large extent independent of location. The best HTC refrigerant in terms of annual costs for Madrid and Paris is R161, whereas both DME and R161 yield almost identical costs for Berlin. In terms of TEWI, DME excels and has the lowest value of all refrigerants studied for all three cities shown in Figure 7. But since the utilization of R161 and DME could be problematic from a safety point of view, the following non-flammable and flammable refrigerants are also of interest: R717 and R152a, which both combine the characteristics of comparatively low costs and low TEWI. A replacement of R161 through R717 or R152a leads to an increase of annual costs of respectively 0.7 to 1.9 % and 0.7 to 0.9 %, while replacement of DME through R717 or R152a causes an increase of TEWI of 2.2 to 2.8 % and 2.8 to 12.8 %, respectively. R32 shows as well promising results regarding costs (increase of 0.8 to 1.1 % compared to the optimal solution). But due to a comparatively high TEWI (up to 61.9 % higher compared to the optimal TEWI in Paris), employment of R32 is discouraged.

5.2. Influence of the cooled space temperature on R744/HTC refrigerant combinations

The choice of a suitable HTC refrigerant may depend on the cooled space temperatures and therefore T_{cool} must be accounted for. For this reason, the

optimization is carried out again at three different T_{cool}.

Figure 10 presents graphically the corresponding results for the city of Paris using R744 in LTC. For a better overview, a subset of only non-flammable and flammable refrigerants is shown in Figure 11a, while highly flammable refrigerants are shown in Figure 11b. Note that R152a is given as a reference in both graphs. As indicated, overcoming a larger temperature difference between T_{amb} and T_{cool} significantly increases both annual cost and TEWI. Taking DME as an example, the annual cost increases from 65 579 € year^{-1} to 105 298 € year^{-1} and the TEWI increases from 261 t to 529 t as the cooled space temperature decreases from −15 °C to −45 °C. This is reasonable, as a larger temperature difference requires more power. Interestingly, in both Figures 11a and 11b, there is only a minimal shift in performance in terms of cost over the temperature range studied. For example, the refrigerant R32 has the lowest annual cost at $T_{cool} = -45$ °C of the subset of only non-flammable and flammable refrigerants. However, at $T_{cool} = -15$ °C, R717 is the optimal HTC refrigerant in terms of both cost and TEWI. It can therefore be concluded that R32 is particularly suitable for very cold applications, while R717 is preferable for cases where the temperature difference is small. However, Figure 10 shows that the performance ranking of each HTC refrigerant in terms of annual cost and TEWI is only slightly dependent on the cooled space temperature T_{cool}.

As shown in Figure 11b, the highly flammable refrigerants all perform particularly well, but overlap, and it is almost impossible to distinguish them visually. For this reason, in the following subsection we focus only on the subset of non-flammable and flammable refrigerants.

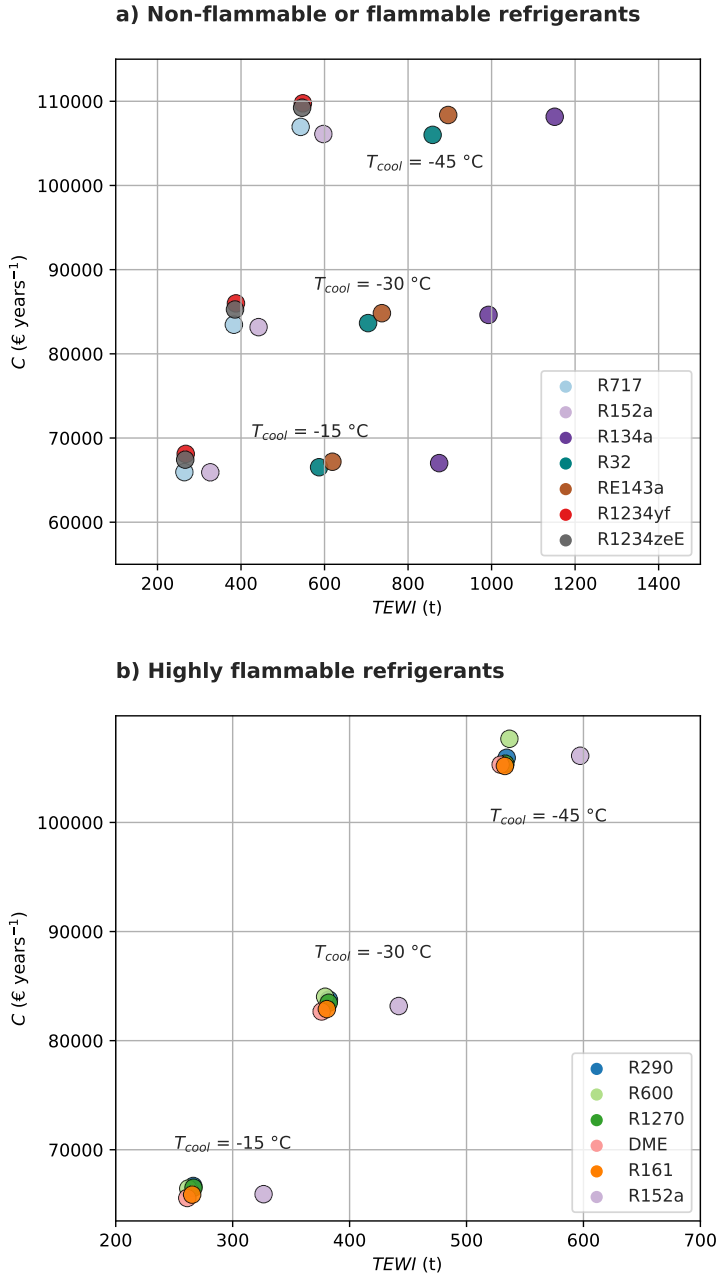

Figure 10: Analysis of a) non-flammable and flammable and b) flammable HTC candidates combined with R744 as LTC fluid at three different T_{cool} ($-45\,°C$, $-30\,°C$ and $-15\,°C$) for Paris.

5.3. Analysis of different LTC refrigerants

In addition to R744, the LTC refrigerants R41 and R170 are also examined. We present the results as combination of LTC and HTC refrigerants, but consider only the subset of non-flammable and flammable HTC refrigerants for better clarity.

5.3.1. Influence of the LTC refrigerant on optimal yearly costs and TEWI

Figure 12 illustrates the results for the city of Paris and given $T_{cool} = -45\,°\mathrm{C}$. As visible, the refrigerant R41 has the best performance in terms of annual costs, followed by R170 and R744. In terms of TEWI, R170 is the best performing LTC refrigerant, followed by R744 and R41. However, for the LTC refrigerants studied, there is only a small variation in annual costs and TEWI of less than 1 % and 5 %, respectively. These differences are therefore much smaller than for the HTC refrigerants presented in the previous section. Therefore, it can be concluded that for the three different refrigerants studied in this paper, the choice of LTC refrigerant has a negligible effect on the overall CRS performance.

5.3.2. Cooled space temperature dependence on the optimal LTC refrigerant

Similar to the R744/HTC refrigerant combinations, the dependence of the LTC refrigerants on T_{cool} must be investigated. For this purpose, combinations of the LTC refrigerants R744, R170 and R41 with the above mentioned subset of non-flammable and flammable HTC refrigerants are investigated. The results of the optimization at three different T_{cool} are visualized in Figure 13 for the city of Paris. At $T_{cool} = -45\,°\mathrm{C}$, the combination of R170/R717 has the lowest TEWI. The R41/R152A combination has the lowest cost, but a slightly higher TEWI. When the temperature is increased from $T_{cool} = -45\,°\mathrm{C}$ to $T_{cool} = -15\,°\mathrm{C}$, there is again a minimal shift: the combination R744/R717 has now the lowest TEWI, while R41/R717 has the lowest annual cost. Both combinations are therefore recommended. Overall, however, it can be said that the influence of the cooled space temperature on the LTC refrigerant selection is as small as on the HTC refrigerant selection.

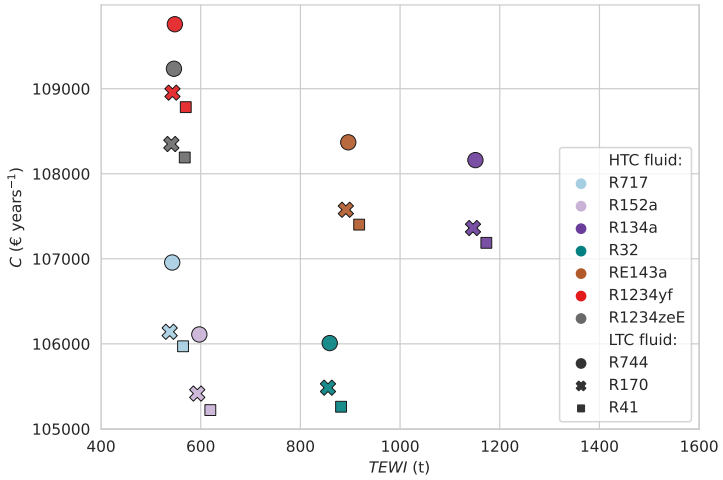

Figure 12: Optimal annual costs for various LTC/HTC refrigerant combinations for Paris at $T_{cool} = -45\,°\mathrm{C}$.

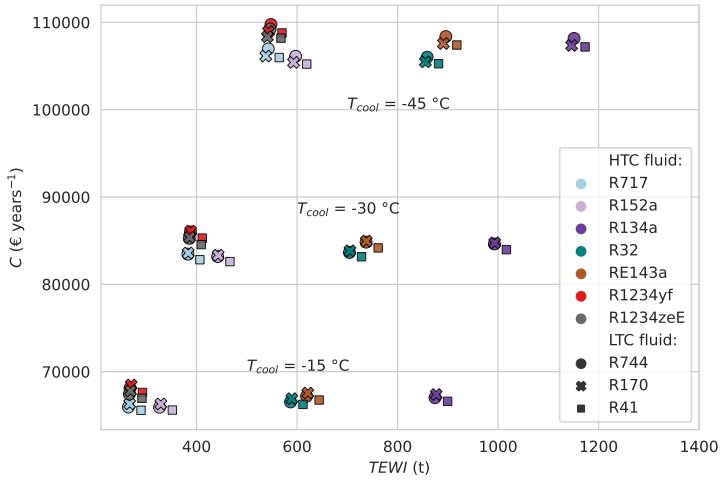

Figure 13: Optimal annual costs for three different T_{cool} ($-45\,°\mathrm{C}$, $-30\,°\mathrm{C}$ and $-15\,°\mathrm{C}$) and three different LTC refrigerants (R744, R170 and R41) for Paris.

6. Conclusion

In this study, a novel methodology for the selection of CRS refrigerant combinations based on a *0D*-steady state thermodynamic model and a bilevel optimization procedure is proposed. The aim is to identify optimal LTC and HTC refrigerants in terms of annual cost and corresponding TEWI based on country specific electricity prices, electricity emission factor and local weather data. Over the year, optimal operation is ensured by maximizing the COP for each ambient temperature as a lower level optimization task. The annual cost is optimized by varying all heat exchanger surfaces as an upper-level optimization task, taking into account the heat transfer within the CRS to obtain realistic results. The proposed methodology is demonstrated by systematically investigating CRS refrigerant combinations for three cities in France, Germany and Spain to reflect the impact of local parameters. Results are reported for Berlin, Madrid and Paris and a cooled space temperature of $T_{cool} = -45\,°\mathrm{C}$. The cooling load is always assumed to be 100 kW. The results can be summarized as follows:

- The same refrigerant combinations yield a high variation of annual costs and TEWI at different locations in Europe. This is due to unlike climate, electricity prices and emission factor. However, these parameters only slightly influence the performance ranking of the refrigerant combinations. This implies that the refrigerant recommendations for the cities studied can be made to a large extent independent of location.

- The comparison of twelve HTC refrigerants at optimal annual costs shows that there is only a small relative variation of annual costs. Regarding TEWI, there is a significant larger variation. The following conclusions can be drawn for the individual refrigerant types:

  - All natural refrigerants perform particular well in terms of TEWI and annual costs, however, most of them are highly flammable. Due to safety considerations, we also consider a set of non-flammable and

flammable refrigerants and recommend some that could serve as substitutes.

  - The investigated HFC show a comparatively wide performance variation regarding TEWI and annual costs. Except for R161 and R152a, they tend to moderate cost rates at comparatively high TEWI, and we discourage the utilization of these refrigerants.
  - HFOs lead to the highest annual cost observed and low TEWI. However, the percentage deviation of the annual costs is not particularly large (3.9 to 4.6 %). Their similar thermodynamic behavior compared to HFCs makes them suitable for a substitution of the latter in already existing or designed CRS.

- The comparison of the three LTC refrigerants at optimal annual cost shows that their impact on overall CRS performance is less than that of the HTC refrigerants for both annual cost and TEWI. However, this may be due to the small set of LTC refrigerants studied and additional research might be needed.

- The dependence of T_{cool} on the optimal HTC and LTC refrigerant selection is in range of $T_{cool} = -45$ to $-15\,°C$ weak and almost negligible. The refrigerant selection can therefore be realized without taking into account T_{cool} in the observed temperature range.

In future work, a safety analysis and an exergy analysis could be incorporated into the refrigerant selection procedure. The economic model could be further developed to either include additional components (e.g. fans and refrigerant cost) or to investigate the impact of a CO_2 tax on the refrigerant ranking. The thermodynamic model should be extended to refrigerant blends and transcritical operation as used in industry. In addition, the steady state model could be transformed into a dynamic model to reflect the fluctuating weather more accurately.

Acknowledgement

This work is supported by the funding of CETHIL, Institute National des Sciences Appliquees de Lyon (INSA-LYON, France). For the purpose of Open Access, a CC-BY public copyright license has been applied by the authors to the present document and will be applied to all subsequent versions up to the Author Accepted Manuscript arising from this submission.

References

[1] Dupont JL, Domanski P, Lebrun P, Ziegler F. The role of refrigeration in the global economy. Informatory Note on Refrigeration Technologies 2019;.

[2] IEA . The future of Cooling. International Energy Agency; 2018. doi:10.1787/9789264301993-en.

[3] Pan M, Zhao H, Liang D, Zhu Y, Liang Y, Bao G. A review of the cascade refrigeration system. Energies 2020;13. doi:10.3390/en13092254.

[4] Lorentzen G. Revival of carbon dioxide as a refrigerant. International Journal of Refrigeration 1994;17(5):292–301. doi:10.1016/0140-7007(94)90059-0.

[5] Duminil M, Domblides JP. Théorie des machines frigorifiques - machine à compression mécanique. cycles multiétagés. Froid industriel 2013;BE 9 732v1:1–24. doi:10.51257/a-v1-be9732.

[6] Adebayo V, Abid M, Adedeji M, Dagbasi M, Bamisile O. Comparative thermodynamic performance analysis of a cascade refrigeration system with new refrigerants paired with co2. Applied Thermal Engineering 2021;184. doi:10.1016/j.applthermaleng.2020.116286.

[7] Aminyavari M, Najafi B, Shirazi A, Rinaldi F. Exergetic, economic and environmental (3e) analyses, and multi-objective optimization of a co2/nh3 cascade refrigeration system. Applied Thermal Engineering 2014;65:42–50. doi:10.1016/j.applthermaleng.2013.12.075.

[8] Rezayan O, Behbahaninia A. Thermoeconomic optimization and exergy analysis of co2/nh3 cascade refrigeration systems. Energy 2011;36:888–95. doi:10.1016/j.energy.2010.12.022.

[9] Getu HM, Bansal PK. Thermodynamic analysis of an r744-r717 cascade refrigeration system. International Journal of Refrigeration 2008;31:45–54. doi:10.1016/j.ijrefrig.2007.06.014.

[10] Deymi-Dashtebayaz M, Sulin A, Ryabova T, Sankina I, Farahnak M, Nazeri R. Energy, exergoeconomic and environmental optimization of a cascade refrigeration system using different low gwp refrigerants. Journal of Environmental Chemical Engineering 2021;9. doi:10.1016/j.jece.2021.106473.

[11] Aktemur C, Ozturk IT, Cimsit C. Comparative energy and exergy analysis of a subcritical cascade refrigeration system using low global warming potential refrigerants. Applied Thermal Engineering 2021;184:116254. URL: https://www.sciencedirect.com/science/article/pii/S1359431120337339. doi:https://doi.org/10.1016/j.applthermaleng.2020.116254.

[12] Blanco Ojeda FWA, Almeida Queiroz MV, Marcucci Pico DF, dos Reis Parise JA, Bandarra Filho EP. Experimental evaluation of low-gwp refrigerants r513a, r1234yf and r436a as alternatives for r134a in a cascade refrigeration cycle with r744. International Journal of Refrigeration 2022;144:175–87. URL: https://www.sciencedirect.com/science/article/pii/S0140700722003000. doi:https://doi.org/10.1016/j.ijrefrig.2022.08.010.

[13] Bellos E, Tzivanidis C. A theoretical comparative study of co2 cascade refrigeration systems. Applied Sciences (Switzerland) 2019;9. doi:10.3390/app9040790.

[14] Lee TS, Liu CH, Chen TW. Thermodynamic analysis of optimal condensing temperature of cascade-condenser in co2/nh3 cascade refriger-

ation systems. International Journal of Refrigeration 2006;29:1100–8. doi:10.1016/j.ijrefrig.2006.03.003.

[15] Sanz-Kock C, Llopis R, Sánchez D, Cabello R, Torrella E. Experimental evaluation of a r134a/co2 cascade refrigeration plant. Applied Thermal Engineering 2014;73:41–50. doi:10.1016/j.applthermaleng.2014.07.041.

[16] Bhattacharyya S, Bose S, Sarkar J. Exergy maximization of cascade refrigeration cycles and its numerical verification for a transcritical co2-c3h8 system. International Journal of Refrigeration 2007;30:624–32. doi:10.1016/j.ijrefrig.2006.11.008.

[17] Gholamian E, Hanafizadeh P, Ahmadi P. Advanced exergy analysis of a carbon dioxide ammonia cascade refrigeration system. Applied Thermal Engineering 2018;137:689–99. URL: https://www.sciencedirect.com/science/article/pii/S135943111736739X. doi:https://doi.org/10.1016/j.applthermaleng.2018.03.055.

[18] Sun Z, Wang Q, Xie Z, Liu S, Su D, Cui Q. Energy and exergy analysis of low gwp refrigerants in cascade refrigeration system. Energy 2019;170:1170–80. URL: https://www.sciencedirect.com/science/article/pii/S0360544218324216. doi:https://doi.org/10.1016/j.energy.2018.12.055.

[19] AIRAH . Methods of calculating Total Equivalent Warming Impact (TEWI) 2012. The Australian Institute of Refrigeration, Air Conditioning and Heating; 2012.

[20] Sánchez D, Cabello R, Llopis R, Catalán-Gil J, Nebot-Andrés L. Energy assessment and environmental impact analysis of an r134a/r744 cascade refrigeration plant upgraded with the low-gwp refrigerants r152a, r1234ze(e), propane (r290) and propylene (r1270). International Journal of Refrigeration 2019;104:321–34. doi:10.1016/j.ijrefrig.2019.05.028.

[21] Mosaffa AH, Farshi LG, Ferreira CAI, Rosen MA. Exergoeconomic and environmental analyses of co2/nh3 cascade refrigeration systems equipped with different types of flash tank intercoolers. Energy Conversion and Management 2016;117:442–53. doi:10.1016/j.enconman.2016.03.053.

[22] Mousavi SA, Mehrpooya M. A comprehensive exergy-based evaluation on cascade absorption-compression refrigeration system for low temperature applications - exergy, exergoeconomic, and exergoenvironmental assessments. Journal of Cleaner Production 2020;246:119005. URL: https://www.sciencedirect.com/science/article/pii/S0959652619338752. doi:https://doi.org/10.1016/j.jclepro.2019.119005.

[23] Mehrpooya M, Mousavi SA, Asadnia M, Zaitsev A, Sanavbarov R. Conceptual design and evaluation of an innovative hydrogen purification process applying diffusion-absorption refrigeration cycle (exergoeconomic and exergy analyses). Journal of Cleaner Production 2021;316:128271. URL: https://www.sciencedirect.com/science/article/pii/S0959652621024860. doi:https://doi.org/10.1016/j.jclepro.2021.128271.

[24] Zhang H, Pan X, Chen J, Xie J. Energy, exergy, economic and environmental analyses of a cascade absorption-compression refrigeration system using two-stage compression with complete intercooling. Applied Thermal Engineering 2023;225:120185. URL: https://www.sciencedirect.com/science/article/pii/S1359431123002144. doi:https://doi.org/10.1016/j.applthermaleng.2023.120185.

[25] Singh KK, Kumar R, Gupta A. Comparative energy, exergy and economic analysis of a cascade refrigeration system incorporated with flash tank (htc) and a flash intercooler with indirect subcooler (ltc) using natural refrigerant couples. Sustainable Energy Technologies and Assessments 2020;39. doi:10.1016/j.seta.2020.100716.

[26] Eini S, Shahhosseini H, Delgarm N, Lee M, Bahadori A. Multi-objective

optimization of a cascade refrigeration system: Exergetic, economic, environmental, and inherent safety analysis. Applied Thermal Engineering 2016;107:804–17. doi:10.1016/j.applthermaleng.2016.07.013.

[27] Patel V, Panchal D, Prajapati A, Mudgal A, Davies P. An efficient optimization and comparative analysis of cascade refrigeration system using nh3/co2 and c3h8/co2 refrigerant pairs. International Journal of Refrigeration 2019;102:62–76. URL: https://www.sciencedirect.com/science/article/pii/S0140700719300970. doi:https://doi.org/10.1016/j.ijrefrig.2019.03.001.

[28] Roy R, Mandal BK. Thermo-economic analysis and multi-objective optimization of vapour cascade refrigeration system using different refrigerant combinations. Journal of Thermal Analysis and Calorimetry 2020;139:3247–61. URL: https://doi.org/10.1007/s10973-019-08710-x. doi:10.1007/s10973-019-08710-x.

[29] Bell IH, Wronski J, Quoilin S, Lemort V. Pure and pseudo-pure fluid thermophysical property evaluation and the open-source thermophysical property library coolprop. Industrial & Engineering Chemistry Research 2014;53(6):2498–508. URL: http://pubs.acs.org/doi/abs/10.1021/ie4033999. doi:10.1021/ie4033999. arXiv:http://pubs.acs.org/doi/pdf/10.1021/ie4033999.

[30] Petter N, Filippo D, Havard R, Arne B. Measurements and experience on semi-hermetic co2 compressors. In: Fifth International Conference on Compressors and Coolants, IIR, Slovak Republic. 2004,.

[31] Stoecker W. Industrial Refrigeration Handbook. Hardcover ed.; McGraw Hill; 1998. ISBN 978-0070616233.

[32] Smith R. Chemical Process Design and Integration. Hardcover ed.; Wiley; 2016. ISBN 978-1119990147.

[33] VRINAT G. Production du froid : technologie des machines industrielles. Froid industriel 1991;URL: https://doi.org/10.51257/a-v1-b2365. doi:10.51257/a-v1-b2365.

[34] Maxwell C. Cost indices. 2023. URL: https://toweringskills.com/financial-analysis/cost-indices/.

[35] Jenkins B. Background for the energy cost calculator. 2014. URL: https://web.archive.org/web/20060708034425/http://faculty.engineering.ucdavis.edu/jenkins/CBC/Calculator/CalculatorBackground.pdf.

[36] Eurostat . Appsso.eurostat.ec.europa.eu. 2022. URL: https://appsso.eurostat.ec.europa.eu/nui/show.do?dataset=nrg_pc_205(%26)lang=en.

[37] Co2 intensity of electricity generation. 2020. URL: https://www.eea.europa.eu/data-and-maps/data/CO2-intensity-of-electricity-generation.

[38] Tsamos K, Ge Y, Santosa I, Tassou S, Bianchi G, Mylona Z. Energy analysis of alternative co2 refrigeration system configurations for retail food applications in moderate and warm climates. Energy Conversion and Management 2017;150:822–9. doi:https://doi.org/10.1016/j.enconman.2017.03.020.

[39] Yilmaz B, Mançuhan E, Yilmaz D. Theoretical analysis of a cascade refrigeration system with natural and synthetic working fluid pairs for ultra low temperature applications. Journal of Thermal Science and Technology 2020;40.

[40] IPCC . Climate Change 2007 - The Physical Science Basis: Working Group I Contribution to the Fourth Assessment Report of the IPCC. Paperback ed.; Cambridge University Press; 2007. ISBN 978-0521705967.

[41] Myhre G, Shindell D, Bréon FM, Collins W, Fuglestvedt J, Huang J, et al. Anthropogenic and natural radiative forcing. Cambridge, UK: Cambridge University Press; 2013, p. 659–740. doi:10.1017/CBO9781107415324.018.

[42] Ammonia: The natural refrigerant of choice (an iiar green paper). 2011. URL: https://web.archive.org/web/20110726172415/https://www.iiar.org/aar/aar_green2.cfm.

[43] Transition to low-gwp alternatives in domestic refrigeration. 2016. URL: https://19january2021snapshot.epa.gov/sites/static/files/2016-12/documents/transitioning_to_low-gwp_alternatives_in_domestic_refrigeration.pdf.

[44] Regulation (eu) no 517/2014 of the european parliament and of the council of 16 april 2014 on fluorinated greenhouse gases and repealing regulation (ec) no 842/2006 text with eea relevance. 2014. URL: https://eur-lex.europa.eu/legal-content/EN/TXT/?uri=uriserv%3AOJ.L_.2014.150.01.0195.01.ENG.

[45] ANSI/ASHRAE 34-2019 - Designation and Safety Classification of Refrigerants. American Society of Heating, Refrigerating and Air-Conditioning Engineers; 2019. URL: https://ashrae.iwrapper.com/ASHRAE_PREVIEW_ONLY_STANDARDS/STD_34_2019.

[46] Roy R, Mandal BK. Energetic and exergetic performance comparison of cascade refrigeration system using r170-r161 and r41-r404a as refrigerant pairs. Heat and Mass Transfer 2018;55(3):723–731. doi:10.1007/s00231-018-2455-7.

[47] Climate.onebuilding.org. 2022. URL: https://climate.onebuilding.org/WMO_Region_6_Europe/default.html.

[48] Virtanen P, Gommers R, Oliphant TE, Haberland M, Reddy T, Cournapeau D, et al. SciPy 1.0: Fundamental Algorithms for Scientific

Computing in Python. Nature Methods 2020;17:261–72. doi:10.1038/s41592-019-0686-2.

[49] Conn AR, Gould NIM, Toint PL. Trust Region Methods. Society for Industrial and Applied Mathematics; 2000. URL: https://epubs.siam.org/doi/abs/10.1137/1.9780898719857. doi:10.1137/1.9780898719857.

[50] Powell MJD. An efficient method for finding the minimum of a function of several variables without calculating derivatives. The Computer Journal 1964;7(2):155–62. URL: https://doi.org/10.1093/comjnl/7.2.155. doi:10.1093/comjnl/7.2.155.

Appendix

Table 8: Results for different HTC refrigerants combinations in Berlin, Madrid and Paris at $T_{cool} = -45\,^{\circ}\mathrm{C}$.

	Berlin		Madrid		Paris	
HTC ref.	C in €year^{-1}	$TEWI$ in t	C in €year^{-1}	$TEWI$ in t	C in €year^{-1}	$TEWI$ in t
R717	143935	3073	110668	2513	106956	543
R290	142080	3009	109707	2469	105925	534
R600	143960	3027	111500	2481	107668	537
R1270	141535	3005	109130	2465	105386	533
DME	141256	2988	108960	2447	105298	529
R1234yf	146715	3090	113814	2537	109758	548
R1234zeE	146059	3076	113198	2523	109235	546
R161	141285	3001	108858	2459	105179	533
R152A	142291	3073	109835	2529	106110	597
R134A	144790	3666	112052	3115	108161	1151
R32	142785	3373	109757	2822	106009	859
RE143a	145033	3413	112279	2862	108370	896